Matter correlations induced by coupling to quantum light

Frank Schlawin and Shaul Mukamel
Department of Chemistry, University of California, Irvine, California 92697-2025, USA
(Received 22 July 2013; published 23 January 2014)

Correlations between uncoupled particles induced by the interaction with different types of light are investigated using a superoperator formalism. We derive compact expressions for the doubly-excited-state distributions of noninteracting multilevel atoms excited by classical laser light, classical stochastic light, and quantum light. We find that the g_2 function of the incoming light can be directly related to its ability to induce correlations in the matter. Unlike coherent light, quantum light can induce entanglement between the atoms. The photon coincidence signal created by classical fields may be factorized into a product of single photon counting rates. This is not the case for quantum light.

DOI: 10.1103/PhysRevA.89.013830 PACS number(s): 42.50.Ct, 42.50.Ex, 03.67.Bg

I. INTRODUCTION

The identification of genuine quantum effects that have no classical counterparts in quantum systems has been a long-standing issue in quantum physics, dating back to the Einstein-Podolsky-Rosen (EPR) paradox, the Bell inequalities, and the hidden-variables theory of Bohm [1,2]. Apart from the very fundamental interest in nonclassical correlations and their possible use as resources for quantum computers [3], methods from quantum information theory have emerged as new tools in nonlinear spectroscopy [4]. Moreover, the possible exploitation of strong correlations in nonlinear spectroscopy with quantum light promises new routes to probe complex quantum systems [5–9]. Quantum spectroscopy offers increased signal strength at low photon fluxes [10–12], new control parameters to disentangle complex spectra [13–16], the control of exciton distributions [17–20], and the suppression of exciton transport [21] thanks to the unusual combination of high temporal and spectral resolution. However, whether all of these effects are genuine quantum effects in the sense that they may not be mimicked—at least in principle—by properly shaped pulses with classical correlations [22–24] remains an open topic. Besides, the interpretation of nonlinear experiments on photosynthetic complexes has ignited a vivid debate about the possible role of quantum coherences in the biological function of these systems [25–27]. Clearly, the induced density matrix of such complex systems upon excitation by coherent laser light or incoherent sunlight is a highly complicated object, and coherence can be induced by other sources such as, e.g., the environment or interactions. In both scenarios, the huge number of free parameters renders a clean interpretation of experiments and even simulations very challenging, and makes it desirable to first discuss these issues in a simpler context, where the influence of the light field can be clearly identified. This study addresses both scenarios by investigating the excited-state density matrices of noninteracting molecules induced by the interaction with light fields.

We consider a collection of N noninteracting molecules ν driven by common external optical fields. By formulating the problem in terms of Liouville space superoperator correlation functions [28], we obtain a compact treatment of the many-body correlations induced by the coupling to the light fields. Using a perturbative expansion in the radiation-matter coupling, observables are given by convolutions of field and matter correlation functions. These correlation functions can be evaluated separately and combined at the end. It is not necessary to solve coupled master equations in the joint field + matter space. We shall use this formalism to calculate the distributions of doubly excited states of noninteracting multilevel atoms induced by the interaction with various kinds of light: classical coherent light, Gaussian stochastic light, separable quantum light, and entangled light. We show that it is possible to excite coherences in the density matrix with stochastic light, as reported in femtosecond measurements with nanosecond pulses in the 1980s [29,30].

Suppose we perform one measurement on each of the observables A_ν, $\nu = 1,\ldots,n$, each acting on the space of molecule ν. We assume a field-matter coupling Hamiltonian of the form $H(t) = E(t)V(t)$, where E and $V = \sum_\nu V_\nu$ denote the electric field and the dipole operators. In the interaction picture, many-body correlation functions are then given by [31]

$$\langle A_{\nu_1}\cdots A_{\nu_k}\rangle = \left\langle \mathcal{T} A_{\nu_1+}\cdots A_{\nu_k+}\exp\left[-\frac{i}{\hbar}\int^t d\tau\, H_-(\tau)\right]\right\rangle, \tag{1}$$

where $\mathcal{T}$ denotes the superoperator time-ordering operator, H is the interaction Hamiltonian, and the superoperators $A_\pm$ are defined by their action on other ordinary operators as follows: $A_\pm X \equiv AX \pm XA$, i.e., A_- is a commutator and A_+ is an anticommutator. If the external laser fields are classical, we can replace electric field operators by c numbers, which allows us to factorize the many-particle correlation function

$$\langle A_{\nu_1}\cdots A_{\nu_k}\rangle = \langle A_{\nu_1}\rangle\cdots\langle A_{\nu_k}\rangle. \tag{2}$$

This factorization reflects the lack of matter correlations in this model; each $\langle A_\nu\rangle$ can be calculated separately in the space of the νth particle. We shall show that quantum (e.g., entangled, or squeezed) light in contrast can induce correlations in matter. A typical term in the perturbative expansion of Eq. (1) in the light-matter coupling is a convolution of field- and matter-superoperator-correlation functions,

$$\int d\tau_1\ldots\int d\tau_k\prod_j\langle \mathcal{T} A_{\nu_j+}V_{\nu_j\pm}(\tau_1')\cdots V_{\nu_j\pm}(\tau_k')\rangle \times\langle \mathcal{T} E(\tau_1')\cdots E(\tau_k')\rangle. \tag{3}$$

Here, the variables $\tau_1' \cdots \tau_k'$ are some permutation of $\tau_1 \cdots \tau_k$. Each matter factor can be calculated in the space of a single molecule, and to arbitrary order in V_-. Because of the nested integrations, the factorization Eq. (2) no longer holds, which implies some degree of correlation between the atoms. Equation (1) represents path integrals in the joint field + particle space, which can substantially affect optical measurements:

It has been suggested in [32] that entangled light can induce collective two-photon resonances between noninteracting two-level atoms. It was argued that the nonseparability of the entangled light wave function directly translates into the nonseparability of the transition amplitude [24,33]. However, it was later shown that these collective resonances are eliminated in measurements performed on single particles such as pump-probe by destructive interference [34]. Matter correlations are nevertheless induced, and can be measured by observables involving more than one atom, such as photon coincidence. These will be studied here. We are interested in entanglement between quasiparticles, i.e., the number of excitations present in the system. Hence, we only consider the subspace composed of one and two excitations. The total Hamiltonian of the system is given by $\mathcal{H} = \otimes_{i=1}^{n} \mathbb{C}^m$, where $\mathbb{C}_i^m$ is the Hilbert space of the ith multilevel atom, and it can be decomposed into

$$\mathcal{H} = \mathbb{S}^{(1)} \oplus \mathbb{S}^{(2)} \oplus \cdots, \tag{4}$$

where $\mathbb{S}^{(k)}$ is the subspace containing k excitations. By denoting the creation operator of an excitation at atom i by $\hat{d}_i$, this means we are interested in the properties of the two-exciton density matrix,

$$\varrho = \sum_{i,j,i',j'} \hat{d}_i^\dagger \hat{d}_j^\dagger |g\rangle\langle g| \hat{d}_{i'} \hat{d}_{j'}. \tag{5}$$

For two-level atoms, $m = 2$, the operators $\hat{d}$ are fermionic operators, and for $m \geqslant 2$ they show some bosonic behavior in the subspaces $\mathbb{S}^{(1)}$ and $\mathbb{S}^{(2)}$. We consider the latter case.

II. TWO-EXCITON DENSITY MATRIX AND PHOTON COINCIDENCE

Assuming that all molecules are initially in the ground state, the density matrix of the interacting matter-field system at time t is given in the interaction picture by the time-ordered exponential

$$\varrho(t) = \mathcal{T} \exp\left[-\frac{i}{\hbar}\int^t d\tau H_-(\tau)\right] |g\rangle\langle g| \otimes \varrho_{\text{field}}, \tag{6}$$

where $|g\rangle$ denotes the ground state of the matter system, and ϱ_{field} denotes the initial state of the light field. To investigate correlations in the matter induced by the interaction with the field, we examine the reduced matter density matrix obtained by tracing out the field degrees of freedom.

The singly excited density matrix is given by the expression

$$\varrho_{i,i'}(t) = \operatorname{tr}\left\{\mathcal{T} \hat{d}_i^\dagger(t)|g\rangle\langle g|\hat{d}_{i'}(t) \exp\left[-\frac{i}{\hbar}\int_{t_0}^t d\tau\, H_-(\tau)\right] \varrho(t_0)\right\}. \tag{7}$$

We shall further examine the doubly excited density matrix, whose elements are given by

$$\varrho_{ij,i'j'}(t) = \operatorname{tr}\left\{\mathcal{T} \hat{d}_i^\dagger(t)\hat{d}_j^\dagger(t)|g\rangle\langle g|\hat{d}_{i'}(t)\hat{d}_{j'}(t) \times \exp\left[-\frac{i}{\hbar}\int_{t_0}^t d\tau\, H_-(\tau)\right] \varrho(t_0)\right\}. \tag{8}$$

In the following, we employ the rotating-wave approximation, and we set $H(t) = V(t)E^\dagger(t) + \text{H.c.}$, where $E^\dagger$ is the negative-frequency component of the electric field and V is the positive-frequency part of the dipole operator,

$$V(t) = \sum_i \mu_{ig} \hat{d}_i e^{-i\omega_{ig}t}. \tag{9}$$

To lowest order in the number of field-matter interactions, Eq. (7) yields

$$\varrho_{i,i'}(t) = \left(-\frac{i}{\hbar}\right)^2 \int^t d\tau_1 \int^t d\tau_1' \times \langle V(\tau_1')\hat{d}_i^\dagger(t)|g\rangle\langle g|\hat{d}_{i'}(t)V^\dagger(\tau_1)\rangle \times \langle E^\dagger(\tau_1')E(\tau_1)\rangle. \tag{10}$$

Similarly, the leading-order contribution to Eq. (8) is given by convolutions of four-point correlation functions. The matter correlation in Eq. (10) factorizes into two transition amplitudes,

$$\langle g|\hat{d}_{i'}(t)V^\dagger(\tau_1)\rangle = \mu_{gi'} e^{-i\omega_{i'g}(t-\tau_1)}. \tag{11}$$

We also introduce the frequency decomposition of the field correlation function,

$$\langle E^\dagger(\tau_1')E(\tau_1)\rangle = \int \frac{d\omega_a}{2\pi} \int \frac{d\omega_b}{2\pi} e^{-i(\omega_b\tau_1 - \omega_a\tau_1')} \langle E^\dagger(\omega_a)E(\omega_b)\rangle, \tag{12}$$

which allows us to carry out the time integrations, and we obtain (see Fig. 1)

$$\varrho_{i,i'}(t) = \left(-\frac{i}{\hbar}\right)^2 \int \frac{d\omega_a}{2\pi} \int \frac{d\omega_b}{2\pi} \mu_{gi'}\mu_{gi} \frac{\langle E^\dagger(\omega_a)E(\omega_b)\rangle e^{i(\omega_a-\omega_b)t}}{(\omega_b - \omega_{ig} + i\epsilon)(\omega_a - \omega_{i'g} - i\epsilon)} \tag{13}$$

$$\varrho_{ij,i'j'}(t) = \left(-\frac{i}{\hbar}\right)^4 \int \frac{d\omega_a}{2\pi} \int \frac{d\omega_b}{2\pi} \int \frac{d\omega_a'}{2\pi} \int \frac{d\omega_b'}{2\pi} \mu_{gi'}\mu_{gj'}\mu_{gi}\mu_{gj} \sum_{\omega_k = \{\omega_{ig}, \omega_{jg}\}} \frac{\langle E^\dagger(\omega_a')E^\dagger(\omega_b')E(\omega_b)E(\omega_a)\rangle e^{-i(\omega_a+\omega_b)t}}{(\omega_a - \omega_k + i\epsilon)(\omega_a + \omega_b - \omega_{ig} - \omega_{jg} + i\epsilon)} \times \sum_{\omega_l = \{\omega_{i'g}, \omega_{j'g}\}} \frac{e^{i(\omega_a'+\omega_b')t}}{(\omega_a' - \omega_l - i\epsilon)(\omega_a' + \omega_b' - \omega_{i'g} - \omega_{j'g} - i\epsilon)}, \tag{14}$$

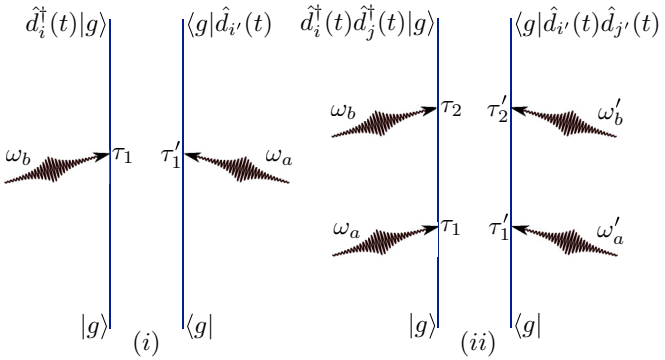

FIG. 1. (Color online) The diagrams representing Eqs. (13) and (14).

where we introduced the infinitesimal imaginary factor ϵ to write the frequency domain Green's function $G_e(\omega) = 1/(\omega - \omega_{eg} + i\epsilon)$. We use the relation

$$\frac{1}{\omega + i\epsilon} = \mathrm{P}\left(\frac{1}{\omega}\right) - i2\pi\delta(\omega), \tag{15}$$

where the δ part yields resonant contributions, and the Cauchy principal value $\mathrm{P}(1/\omega)$ gives positive and negative contributions outside the resonance. Due to cancellations, they are typically small but not necessarily negligible (in the Lamb shift calculation, they diverge [35]). Formally, this implies that the numerators in Eqs. (13) and (14) are analytic, and have no poles. Below, we shall neglect the principal value. In Fig. 5 we will demonstrate that this is justified in the present applications. Equation (14) then yields the Fourier transform of the field correlation function,

$$\varrho_{ii'}(t) = \left(-\frac{i}{\hbar}\right)^2 \mu_{gi'}\mu_{gi} e^{i(\omega_{i'g}-\omega_{ig})t} \times \langle E^\dagger(\omega_{i'g})E(\omega_{ig})\rangle, \tag{16}$$

$$\varrho_{ij,i'j'}(t) = \left(-\frac{i}{\hbar}\right)^4 \mu_{gi'}\mu_{gj'}\mu_{gi}\mu_{gj} e^{-i(\omega_{ig}+\omega_{jg}-\omega_{i'g}-\omega_{j'g})t} \times \langle E^\dagger(\omega_{i'g})E^\dagger(\omega_{j'g})E(\omega_{ig})E(\omega_{jg})\rangle. \tag{17}$$

Note also that the simple form of Eqs. (16) and (17) only holds provided the free time evolution of the matter is unitary. Dissipation would complicate the picture.

A good measure of these density matrices is provided by the two-photon counting signal

$$S_{ij}(\Gamma) = \frac{\langle A_i(t)A_j(t)\rangle}{\langle A_i(t)\rangle\langle A_j(t)\rangle}, \tag{18}$$

with $A_i(t) = \hat{d}^\dagger(t)|g\rangle\langle g|\hat{d}(t)$, and Γ denoting the set of control parameters. We collect photons from the multilevel atoms, which we assume to be distinguishable by their frequency. A nonvanishing S_{ij} implies that the multilevel atoms are correlated; the probability of the system i and j being excited differs from the product of probabilities. The photon coincidence results can be obtained directly from Eq. (17),

$$S_{ij}(\Gamma) = \frac{\langle E^\dagger(\omega_{ig})E^\dagger(\omega_{jg})E(\omega_{ig})E(\omega_{jg})\rangle}{\langle E^\dagger(\omega_{ig})E(\omega_{ig})\rangle\langle E^\dagger(\omega_{jg})E(\omega_{jg})\rangle}. \tag{19}$$

Equation (19) is similar—but not identical—to the Fourier transform of the g_2 function of the incoming fields [36],

$$g_2(t,\tau) \equiv \frac{\langle E^\dagger(t)E^\dagger(t+\tau)E(t+\tau)E(t)\rangle}{\langle E^\dagger(t)E(t)\rangle^2}. \tag{20}$$

To see the difference between the two quantities, we just note that the frequency decomposition of the nominator of Eq. (20) is given by

$$\begin{aligned}&\langle E^\dagger(t)E^\dagger(t+\tau)E(t+\tau)E(t)\rangle \\ &= \int\frac{d\omega_a'}{2\pi}\int\frac{d\omega_b'}{2\pi}\int\frac{d\omega_a}{2\pi}\int\frac{d\omega_b}{2\pi} \\ &\quad\times\langle E^\dagger(\omega_a')E^\dagger(\omega_b')E(\omega_b)E(\omega_a)\rangle \\ &\quad\times e^{i(\omega_a'+\omega_b'-\omega_b-\omega_a)t}e^{i(\omega_b'-\omega_b)\tau},\end{aligned} \tag{21}$$

and cannot be brought into the form of Eq. (19). Still, the ability of the incoming light to induce correlation between noninteracting multilevel atoms is closely connected to its g_2 function. In the following, we will explore this relation for various kinds of light.

III. CLASSICAL LIGHT

A. Coherent light

For classical coherent light, we can factorize the electric-field operators of the four-point correlation function $\langle E^\dagger(\omega_{ig})E^\dagger(\omega_{jg})E(\omega_{i'g})E(\omega_{j'g})\rangle$ into field amplitudes $F^*(\omega_{ig})F^*(\omega_{jg})F(\omega_{i'g})F(\omega_{j'g})$. The density matrix then factorizes into products of single-photon transition amplitudes

$$\varrho_{ij,i'j'}(t) = T_i^*(t)T_j^*(t)T_{j'}(t)T_{i'}(t), \tag{22}$$

with

$$T_i(t) = \left(-\frac{i}{\hbar}\right)\mu_{ig}F(\omega_{ig})e^{-i\omega_{ig}t}. \tag{23}$$

This is a product state, and all many-body observables will factorize as in Eq. (2), signifying the absence of correlations.

We illustrate this for a simple system of six multilevel atoms with energies between $\omega_{e_1g} = 1.47$ eV and $\omega_{e_6g} = 1.543$ eV. All density matrices are normalized to $\mathrm{tr}[\varrho] = 1$. We start with coherent light with a Gaussian envelope,

$$F(\omega) = \exp\left(-\frac{(\omega-\omega_0)^2}{2\sigma_1^2}\right). \tag{24}$$

The absolute value of the density matrices is shown in Fig. 2. The excitation probability of any doubly excited state can be directly traced back to the overlap of the pulse's power spectrum with the multilevel atom energies. For instance, state $|16\rangle$ is always weakly excited in our current scheme, since the two energies are far detuned from one another, and cannot be efficiently excited by a single laser pulse.

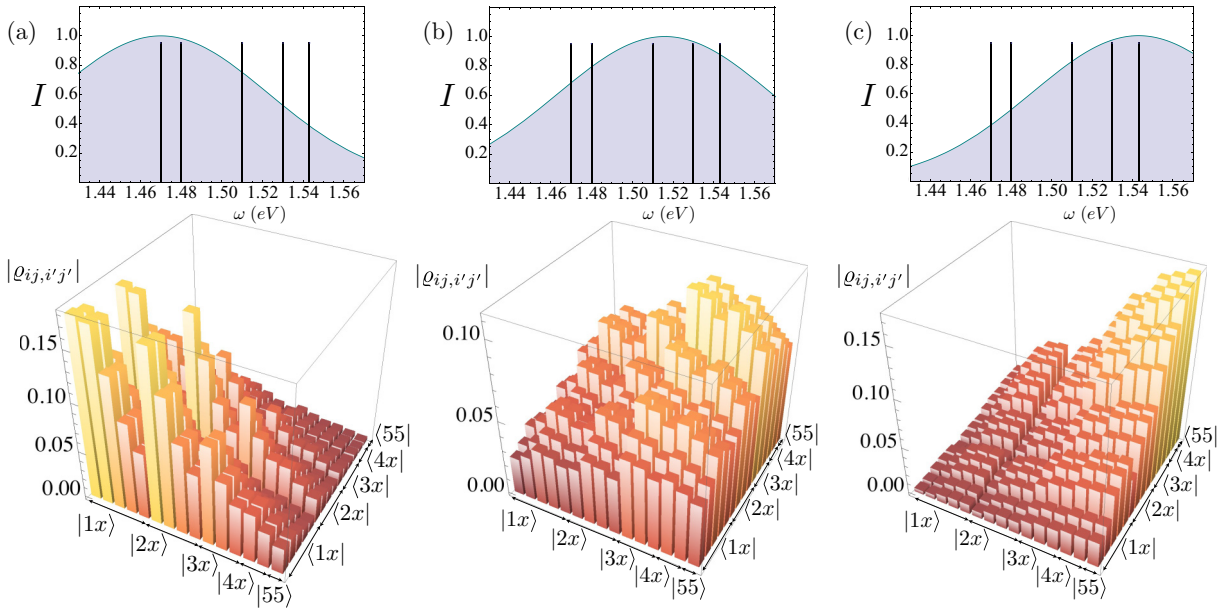

FIG. 2. (Color online) The top panels depict the power spectra of the light in arbitrary units; it has a bandwidth $\sigma_1 = 0.14$ eV. The central frequency of the light beam is varied between 1.47 eV (a), 1.516 eV (b), and 1.543 eV (c). The energies of the multilevel atoms are indicated by black lines. The bottom plots show the absolute value of the density matrices induced by coherent light [Eq. (22)]. The states are indicated as $|1x\rangle \hat{=} |12\rangle, \ldots, |16\rangle$, $|2x\rangle \hat{=} |23\rangle, \ldots, |26\rangle$, etc.

Due to the factorization (22), we obtain for the coincidence rate

$$S_{ij}(\Gamma) = 1. \tag{25}$$

This reflects the absence of correlations between the multilevel atoms; we obtain the identical result for the g_2 function.

B. Stochastic light

For stochastic light, the expectation value in the four-point correlation function $\langle E^*(\omega_{ig})E^*(\omega_{jg})E(\omega_{i'g})E(\omega_{j'g})\rangle$ denotes an average with respect to the realizations of the complex random (classical) variable $E(\omega)$. In the following, we will assume Gaussian stochastic light. This is a common model if we take many degrees of freedom (i.e., modes) into account, as it can be rationalized by the central limit theorem [35]. The correlation function then factorizes into two-point functions [37]

$$\begin{aligned}\langle E^*(\omega_{ig})E^*(\omega_{jg})E(\omega_{i'g})E(\omega_{j'g})\rangle &= \langle E^*(\omega_{ig})E(\omega_{j'g})\rangle\langle E^*(\omega_{jg})E(\omega_{i'g})\rangle \\ &\quad + \langle E^*(\omega_{ig})E(\omega_{i'g})\rangle\langle E^*(\omega_{jg})E(\omega_{j'g})\rangle. \end{aligned}\tag{26}$$

We shall represent the two-point correlation function in the form

$$\langle E^*(\omega')E(\omega)\rangle = F^*(\omega')F(\omega)C(\omega-\omega'), \tag{27}$$

where $F(\omega)$ denotes the field amplitude, and the correlation term $C(\omega-\omega') = C(\omega'-\omega)$ describes the degree of stochasticity. By substituting Eqs. (26) and (27) into Eq. (17), we obtain

$$\begin{aligned}\varrho_{ij,i'j'}(t) = \mu_{gi}\mu_{gj}\mu_{gi'}\mu_{gj'}\left(-\frac{i}{\hbar}\right)^4 F(\omega_{e'_ig})F(\omega_{e'_jg})F^*(\omega_{ig})F^*(\omega_{jg})e^{-i(\omega_{e'_ig}+\omega_{e'_jg}-\omega_{ig}+\omega_{jg})t} \\ \times [C(\omega_{e'_ig}-\omega_{ig})C(\omega_{e'_jg}-\omega_{jg}) + C(\omega_{e'_ig}-\omega_{jg})C(\omega_{e'_jg}-\omega_{ig})].\end{aligned}\tag{28}$$

For $C(\omega) \to 1$, we recover the fully coherent light result of the previous section, which factorizes into the product of single-photon transition amplitudes, as expected from the previous discussion. In the opposite, white noise, limit, $C(\omega) \to \delta(\omega)$, the off-diagonal density matrix elements vanish, and the resulting state is an incoherent mixture of populations. This is illustrated in Fig. 3 for the same model system described in the previous section. We chose a Gaussian envelope for the frequency correlation function in Eq. (28),

$$C(\omega-\omega') = \left(-\frac{(\omega-\omega')^2}{2\sigma_2^2}\right). \tag{29}$$

The dependence on C is shown in Fig. 3 for different values of σ_2. For very large σ_2, i.e., weak stochasticity, the density matrix in Fig. 3(a) is almost identical to the density matrix excited by coherent light with the same parameters in Fig. 2(b). But with an increasing degree of stochasticity, the off-diagonal elements are suppressed, and only the populations survive in Fig. 3(c).

We next turn to the coincidence rate. According to Eq. (26), it yields

$$S_{ij}(\Gamma) = 1 + \frac{\langle E^*(\omega_{ig})E(\omega_{jg})\rangle\langle E^*(\omega_{jg})E(\omega_{ig})\rangle}{\langle E^*(\omega_{ig})E(\omega_{ig})\rangle\langle E^*(\omega_{jg})E(\omega_{jg})\rangle}. \tag{30}$$

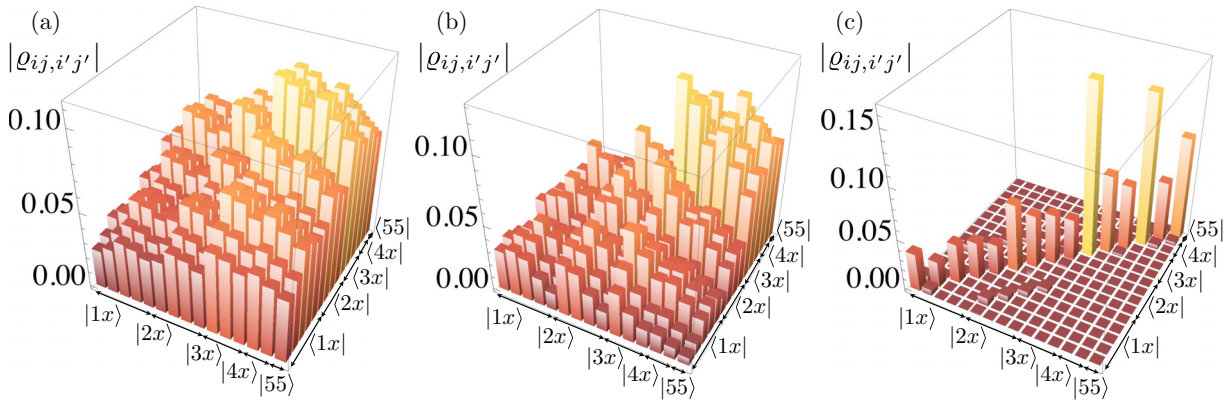

FIG. 3. (Color online) The absolute value of the density matrix [Eq. (28)] is depicted for (a) $\sigma_1 = 0.14$ eV and $\sigma_2 = 0.5$ eV, (b) $\sigma_2 = 0.05$ eV, and (c) $\sigma_2 = 0.005$ eV.

The first line of Eq. (26) yields the factor 1. The second line in (26) gives rise to the second term, and can in principle yield new information. Let us use the two-point correlation function (27) to explore the limiting behavior of Eq. (30). For $C(\omega) \to \delta(\omega)$, the second term vanishes, and we obtain $S_{ij}(\Gamma) = 1$. On the other hand, when $C(\omega) \to 1$, the correlators factorize into field amplitudes, and the second term becomes 1, such that we end up with $S_{ij}(\Gamma) = 2$. This behavior is reminiscent of the behavior of the g_2 function of stationary stochastic light, which is given by $g_2(0) = 2$ and $g_2(\tau) \to 1$ for $\tau \gg \tau_c$ [36], where τ_c denotes the correlation time.

IV. SUPERPOSITIONS OF TWO-PHOTON FOCK STATES

A general two-photon state of the radiation field can be written as

$$|\psi\rangle = \int d\omega_a \int d\omega_b \Phi(\omega_a,\omega_b) a^\dagger(\omega_a) a^\dagger(\omega_b)|0\rangle. \quad (31)$$

If the spectral two-photon amplitude $\Phi(\omega_a,\omega_b)$ can be factorized, i.e., $\Phi(\omega_a,\omega_b) = \Phi_1(\omega_a)\Phi_2(\omega_b)$, the state is separable, otherwise it is time-frequency entangled [38,39].

We use the following representation of the electric field:

$$E(t) = \mathcal{A}(\omega_i) \int d\omega\, e^{-i\omega t} a(\omega), \quad (32)$$

where $\mathcal{A}(\omega_i)$ is the central frequency of the ith beam, which does not depend strongly on this frequency, and the photon annihilation operators satisfy $[a(\omega),a^\dagger(\omega')] = \delta(\omega - \omega')$. In this case, the four-point field correlation function factorizes as

$$\langle E^\dagger(\omega_a') E^\dagger(\omega_b') E(\omega_b) E(\omega_a)\rangle$$
$$= \langle E^\dagger(\omega_a') E^\dagger(\omega_b')\rangle \langle E(\omega_b) E(\omega_a)\rangle \quad (33)$$
$$= \mathcal{A}^*(\omega_a')\mathcal{A}^*(\omega_b')\mathcal{A}(\omega_b)\mathcal{A}(\omega_a)\Phi^*(\omega_a',\omega_b')\Phi(\omega_a,\omega_b). \quad (34)$$

Equation (10) now factorizes into two-photon transition amplitudes [40,41],

$$\varrho_{ij,i'j'}(t) = T_{ij}^*(t) T_{i'j'}(t), \quad (35)$$

with

$$T_{ij}(t) = \mathcal{A}(\omega_1)\mathcal{A}(\omega_2)\mu_{gi}\mu_{gj}\, e^{-i(\omega_{ig}+\omega_{jg})t} \times [\Phi(\omega_{ig},\omega_{jg}) + \Phi(\omega_{jg},\omega_{ig})]. \quad (36)$$

This means that two-photon states prepare pure doubly excited states, just like classical coherent light, Eq. (22). However, even if the two-photon state is separable, $\Phi(\omega_a,\omega_b) = \Phi_1(\omega_a)\Phi_2(\omega_b)$, we obtain

$$T_{ij}(t) = \mathcal{A}(\omega_1)\mathcal{A}(\omega_2)\mu_{gi}\mu_{gj}\, e^{-i(\omega_{ig}+\omega_{jg})t} \times [\Phi_1(\omega_{ig})\Phi_2(\omega_{jg}) + \Phi_1(\omega_{jg})\Phi_2(\omega_{ig})]. \quad (37)$$

If $\Phi_1 = \Phi_2$, i.e., the two photons are indistinguishable, the two terms are identical, and the transition amplitude factorizes into the product of single-photon transition amplitudes as in Eq. (22). In general, however, we may not factorize (36) into such a product, $T_{ij} \neq T_i T_j$. The absorption of a photon from beam 1 by molecule i depletes this field, leaving only beam 2 to excite molecule j. Thus, even though the photon wave function is separable, it can create an entangled doubly excited state of the matter. This argument can be straightforwardly extended to general N-photon Fock states.

Figure 4 shows the density matrices created by twin photons with the two-photon wave function [42–45]

$$\Phi(\omega_a,\omega_b) = \exp\left(-\frac{(\omega_a+\omega_b-\omega_1-\omega_2)^2}{2\sigma^2}\right) \times \mathrm{sinc}[(\omega_a-\omega_1)T_1/2 + (\omega_b-\omega_2)T_2/2]. \quad (38)$$

Here, ω_1 and ω_2 are the central frequencies of the two beams, σ denotes the pump pulse envelope, and T_1 and T_2 are time scales that are given by group velocities inside the birefringent crystal, where the entangled photons are created. In all three cases, the power spectrum of the entangled beams is roughly equal to that of the coherent pulses in Fig. 2. The pump bandwidth σ, which controls the frequency entanglement between the photons, is varied in Figs. 4(a)–4(c). As σ is decreased, individual doubly excited states can be excited, even though the bandwidth of the individual beams remains constant [17].

Equation (34) implies that the two-photon coincidence can be written as the modulus square of a two-photon transition amplitude,

$$\langle A_i(t) A_j(t)\rangle = \left|\left(-\frac{i}{\hbar}\right)^2 \mu_{ig}\mu_{jg}[\Phi(\omega_{ig},\omega_{jg}) + \Phi(\omega_{jg},\omega_{ig})]\right|^2, \quad (39)$$

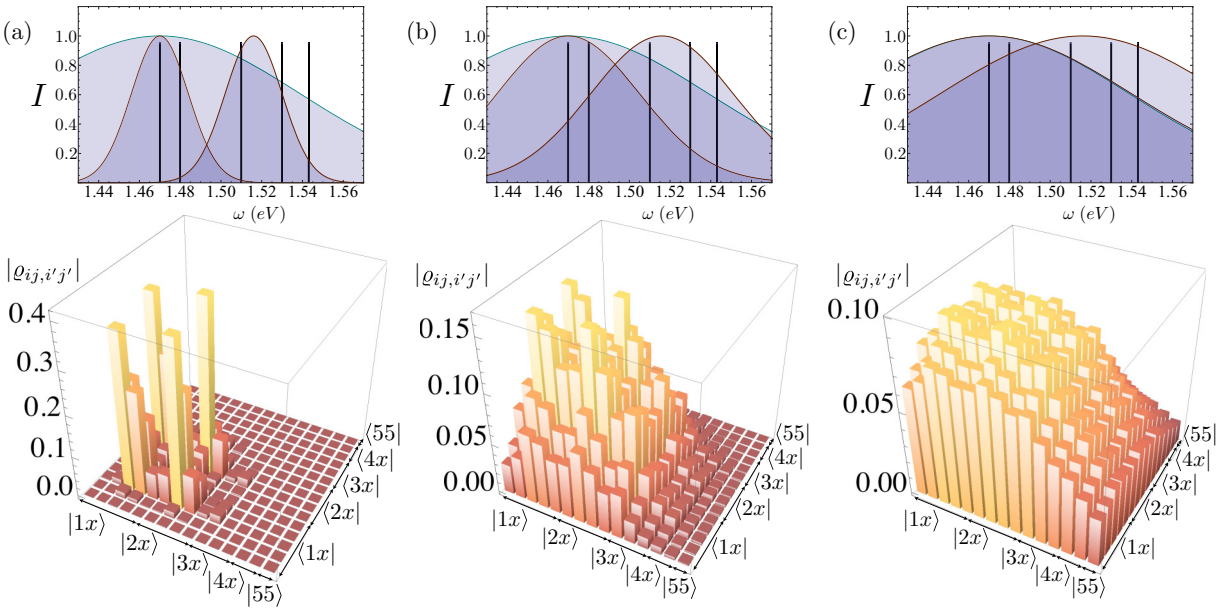

FIG. 4. (Color online) The top panels depict exponentials with the entanglement time bandwidth (blue) and the pump bandwidth (red) centered around the two central frequencies of the entangled photons. (a) The absolute value of the density matrix created by twin photons [Eqs. (36) and (38)] with $\omega_1 = 1.47$ eV, $\omega_2 = 1.516$ eV, $T_2 - T_1 = 0.07$ 1/eV, and $\sigma = 0.014$ eV. (b) Same as (a) for $\sigma = 0.03$ eV. (c) Same as (a) for $\sigma = 0.07$ eV.

whereas the single-particle measurement is given by

$$\langle A_i(t)\rangle = \left(-\frac{i}{\hbar}\right)^2 \mu_{ig}^2 \int d\omega |\Phi(\omega_{ig},\omega) + \Phi(\omega,\omega_{ig})|^2. \quad (40)$$

Two-photon coincidence depends on the full two-photon wave function, whereas the single-particle measurement only depends on the marginal, where one frequency is integrated out. Energy entanglement can create strong correlations between the two frequencies ω_{ig} and ω_{jg}, which are destroyed by the integration in Eq. (40). Thus, Eq. (19) can be manipulated by the control parameters of the twin state (38).

It is also well known that this state can exhibit photon antibunching [35], i.e., $g_2(\tau) \geqslant g_2(0)$, which is impossible with classical light.

A. Numerical integration

The convergence of the integral of Eqs. (14)–(17) is demonstrated in Fig. 5. As ϵ is decreased, the density matrix converges to the approximate solution given by Eqs. (16) and (17). For a finite dephasing rate ϵ, the Lorentzians in Eq. (14) cannot be replaced by δ functions. As a measure of the difference between the two matrices, we employ the trace distance [46]

$$\mathcal{D}(\varrho,\varrho') \equiv \tfrac{1}{2}|\sqrt{(\varrho-\varrho')^2}|, \quad (41)$$

where the trace norm $|\varrho| = \mathrm{tr}\{\varrho\}$ is used, and the two matrices are given by Eqs. (14) and (17), respectively. This is plotted in Fig. 6, and it can be clearly seen that the trace distance approaches zero as ϵ is decreased.

V. MIXED STATE OF THE RADIATION FIELD; THERMAL LIGHT

We have seen that quantum light can entangle different TLAs. Even though state (31) itself is not entangled, the lack of information about which TLA absorbs which photon causes the entanglement of the two atoms. To establish that

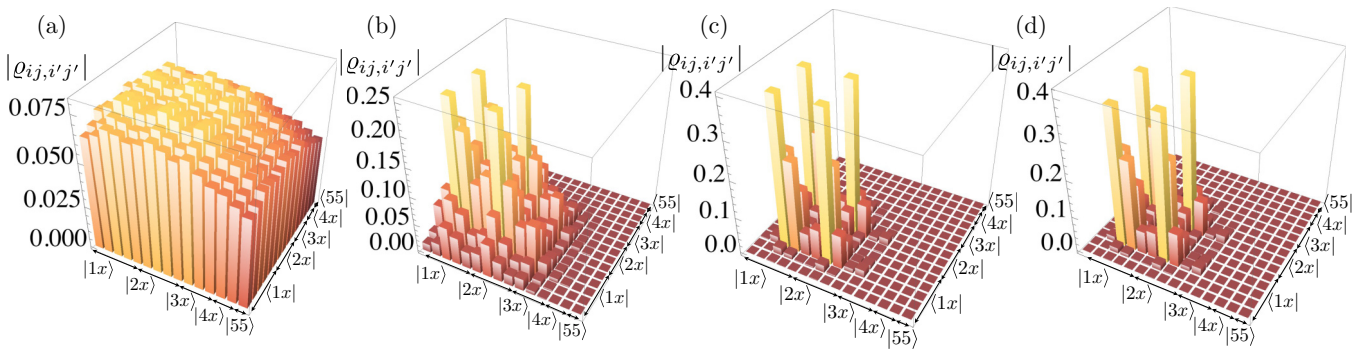

FIG. 5. (Color online) (a) The absolute value of the density matrix created by entangled light according to Eq. (14) with $\epsilon = 0.1$ eV. (b) Same as (a) for $\epsilon = 0.01$ eV. (c) Same as (a) for $\epsilon = 0.0001$ eV. (d) The absolute value according to Eq. (17).

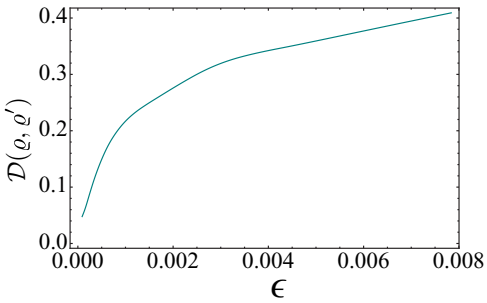

FIG. 6. (Color online) The trace distance (41) between the doubly excited density matrices (14) and (17) is plotted vs the imaginary factor ϵ.

the quantum coherence of the pure state (31) is essential for the entanglement, we now consider an incoherent mixture of two-photon states, described by the density matrix

$$\varrho_{\rm field} = \int d\omega_a \int d\omega_b |\Phi_1(\omega_a)|^2 |\Phi_2(\omega_b)|^2 \times a^\dagger(\omega_a) a^\dagger(\omega_b)|0\rangle\langle 0|a(\omega_a)a(\omega_b) \tag{42}$$

with frequency distributions $|\Phi_1|^2$ and $|\Phi_2|^2$. Using Eqs. (17) and (42), this yields for the doubly excited density matrix

$$\varrho_{ij,i'j'}(t) = |\Phi_1(\omega_{i'g})|^2 |\Phi_2(\omega_{j'g})|^2 |\mathcal{A}(\omega_1)|^2 |\mathcal{A}(\omega_2)|^2 \times [\delta(\omega_{ig}-\omega_{i'g})\delta(\omega_{jg}-\omega_{j'g}) + \delta(\omega_{ig}-\omega_{j'g})\delta(\omega_{jg}-\omega_{i'g})]. \tag{43}$$

Off-diagonal elements vanish, and the final density matrix consists of a classical mixture of uncorrelated doubly excited states. Photon coincidence measurements then yield

$$S_{ij}(\Gamma) = 1 + \delta(\omega_{ig}-\omega_{jg}), \tag{44}$$

which is identical to the white noise limit in Eq. (30).

A. Thermal light

The density matrix of thermal light is given by [37]

$$\varrho_{\rm th} = \int d\omega \sum_{n(\omega)=0}^{\infty} f_n(\omega)|n(\omega)\rangle\langle n(\omega)|, \tag{45}$$

$$f_n(\omega) = e^{-\hbar\omega n/(k_B T)}[1 - e^{-\hbar\omega/(k_B T)}]. \tag{46}$$

The four-point correlation function is then given by

$$\begin{aligned}
&\langle E^\dagger(\omega_a')E^\dagger(\omega_b')E(\omega_b)E(\omega_a)\rangle \\
&= \{[1-\delta(\omega_a-\omega_b)]\delta(\omega_a'-\omega_a)\delta(\omega_b'-\omega_b) + [1-\delta(\omega_a-\omega_b)]\delta(\omega_a'-\omega_b)\delta(\omega_b'-\omega_a)\} \\
&\quad\times |\mathcal{A}(\omega_a)|^2 \sum_{n(\omega_a)=0}^{\infty} f_n(\omega_a)n(\omega_a)\ |\mathcal{A}(\omega_b)|^2 \sum_{n(\omega_b)=0}^{\infty} f_n(\omega_b)n(\omega_b) \\
&\quad+ \delta(\omega_a-\omega_b)\delta(\omega_a'-\omega_a)\delta(\omega_b'-\omega_b)|\mathcal{A}(\omega_a)|^4 \sum_{n(\omega_a)=0}^{\infty} f_n(\omega_a)n(\omega_a)[n(\omega_a)-1]
\end{aligned} \tag{47}$$

$$\begin{aligned}
&= \{[1-\delta(\omega_a-\omega_b)]\delta(\omega_a'-\omega_a)\delta(\omega_b'-\omega_b) + [1-\delta(\omega_a-\omega_b)]\delta(\omega_a'-\omega_b)\delta(\omega_b'-\omega_a)\}\frac{|\mathcal{A}(\omega_a)|^2}{e^{x_a}-1}\frac{|\mathcal{A}(\omega_b)|^2}{e^{x_b}-1} \\
&\quad+ \delta(\omega_a-\omega_b)\delta(\omega_a'-\omega_a)\delta(\omega_b'-\omega_b)|\mathcal{A}(\omega_a)|^4\left[\frac{1}{4}\frac{\cosh(x_a/2)}{\sinh^2(x_a/2)} - \frac{1}{e^{x_a}-1}\right],
\end{aligned} \tag{48}$$

where we defined $x_i = \hbar\omega_a/(k_B T)$. Just as in the two-photon case, the density matrix induced by thermal light shows no coherences either. We obtain for the coincidence measurements

$$S_{ij}(\Gamma) = [1-\delta(\omega_{ig}-\omega_{jg})] + \delta(\omega_{ig}-\omega_{jg}) \times [\cosh(x_i/2)e^{x_i/4} - (e^{x_i}-1)]. \tag{49}$$

For our system, $\omega_{ig} \neq \omega_{jg}$, and therefore the second term vanishes, and we obtain the same result as with stochastic light in the white noise limit. But in general, the second term exists and has to be taken into account.

VI. SQUEEZED LIGHT

Two-photon Fock states as discussed in Sec. V represent an idealized case in the limit of a weak pump pulse. When the pump intensity is increased, photon pairs from different downconversion events overlap in time. These quantum states are squeezed in their collective quadrature fluctuations [47,48]. We employ the theory developed in [49–51] to derive the density matrices created by these states. The field correlation function in Eq. (17) is given by three terms,

$$\begin{aligned}
&\langle E^\dagger(\omega_{ig})E^\dagger(\omega_{jg})E(\omega_{i'g})E(\omega_{j'g})\rangle \\
&= \langle E^\dagger(\omega_{ig})E^\dagger(\omega_{jg})\rangle\langle E(\omega_{i'g})E(\omega_{j'g})\rangle \\
&\quad+ \langle E^\dagger(\omega_{ig})E(\omega_{i'g})\rangle\langle E^\dagger(\omega_{jg})E(\omega_{j'g})\rangle \\
&\quad+ \langle E^\dagger(\omega_{ig})E(\omega_{j'g})\rangle\langle E^\dagger(\omega_{jg})E(\omega_{i'g})\rangle.
\end{aligned} \tag{50}$$

The first line in Eq. (50) has the same structure as Eq. (34), $\langle E^\dagger E^\dagger E E\rangle = \langle E^\dagger E^\dagger\rangle\langle E E\rangle$. It correlates the two absorption events and shows the same kind of physics as discussed in the previous sections. The second and third lines, on the other hand, have the same structure as the correlation function of

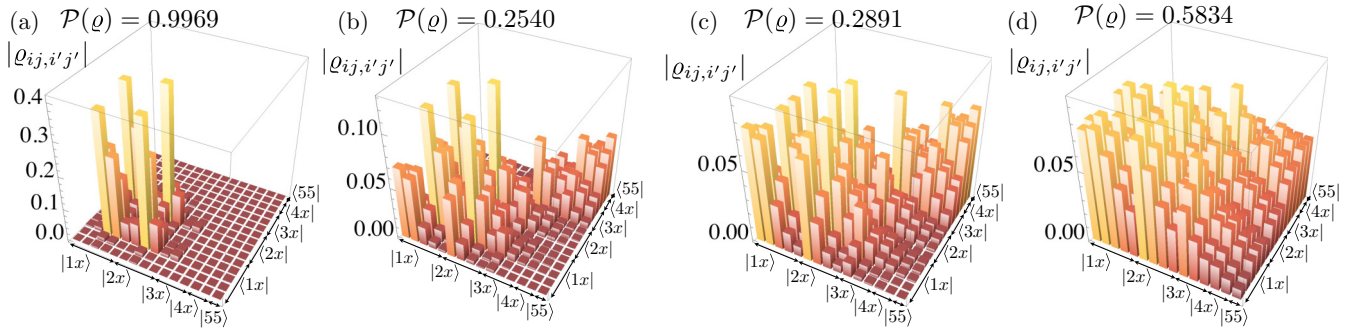

FIG. 7. (Color online) (a) The absolute value of the density matrix created by squeezed light [Eq. (50)] with $\omega_1 = 1.47$ eV, $\omega_2 = 1.516$ eV, $T_2 - T_1 = 0.07$ 1/eV, and $\sigma = 0.014$ eV. The pump intensity (in units of $\hbar$) is set to $|\alpha|^2 = 1$. (b) Same as (a) for $|\alpha|^2 = 2500$. (c) Same as (a) for $|\alpha|^2 = 10\,000$. (d) Same for $|\alpha|^2 = 90\,000$. We also show the purity of each matrix, defined by $\mathcal{P}(\varrho) = \mathrm{tr}\{\varrho^2\}$.

Gaussian stochastic light, $\langle E^\dagger E\rangle\langle E^\dagger E\rangle$. As shown in [51], the first line dominates for low pump intensities, and with increasing intensity we can observe a crossover between the two contributions.

Figure 7 shows the density matrices for different pump intensities. For low pump intensities, the matrix in Fig. 7(a) looks very similar to the one induced by the two-photon Fock state in Fig. 4(c). Just like in the two-photon case, the pump bandwidth determines the selectivity of doubly excited states. But when the intensity is increased, the autocorrelation contributions become stronger. They are controlled by the much larger bandwidth of the individual beams. Hence, the selectivity is lost, and all the states get excited.

We also note that, whereas the two-photon state excites pure doubly excited states, the autocorrelation contribution leads to the excitation of mixed states. Figure 7 reveals that the purity changes nonmonotonically with increasing pump intensity. To further explore this behavior, we plot the purity versus the pump intensity in Fig. 8(a) for different entanglement times (i.e., different bandwidths of the individual beams). The can distinguish two different kinds of behavior: the green and the blue plots are created by broadband squeezed light, where the sum of the individual beams is much larger than the pump bandwidth. They show a pronounced minimum of the purity at $\mathcal{P} \approx 0.3$ and 0.4, respectively, and an increase to $\mathcal{P} \approx 0.6$ for higher intensities. The red and the gray plots correspond to beams with weak frequency entanglement, where the bandwidth of the individual beams is of a similar size to the pump bandwidth. These states do not show a pronounced minimum, instead their purity decreases monotonically with increasing pump intensity. To explain these differences, we define the relative weight of the coherent contribution [i.e., the first line of Eq. (50)] and of the incoherent contribution (the second and third lines) by the ratio $w(|\alpha|^2) = \mathrm{tr}\{\varrho_{\mathrm{coh}}\}/\mathrm{tr}\{\varrho\}$, where ϱ_{coh} is created by the coherent contribution of Eq. (50),

$$\varrho_{\mathrm{coh},\,ij,i'j'} = \left(-\frac{i}{\hbar}\right)^4 \mu_{gi'}\mu_{gj'}\mu_{gi}\mu_{gj} e^{i(\omega_{ig}+\omega_{jg}-\omega_{i'g}-\omega_{j'g})t} \times \langle E^\dagger(\omega_{ig})E^\dagger(\omega_{jg})\rangle\langle E(\omega_{i'g})E(\omega_{j'g})\rangle, \quad (51)$$

and accordingly ϱ_{incoh} is created by the incoherent contribution. These quantities are plotted in Figs. 8(b) and 8(c) together with the purity of the full state versus the pump intensity. With increasing intensity, the incoherent contribution becomes stronger, and eventually dominates. Clearly, the crossover happens for much smaller intensity in the broadband case [Fig. 8(b)]. The broad bandwidth allows the incoherent contribution to access all the doubly excited states, whereas the coherent part is restricted to a subset due to the frequency entanglement [see Fig. 7(a)]. The inset in Fig. 8(b) depicts the purity of ϱ_{incoh} versus the pump intensity. Its increase with the pump intensity in combination with the crossover between coherent and incoherent contribution accounts for the nonmonotonic behavior of the purity of the full density matrix.

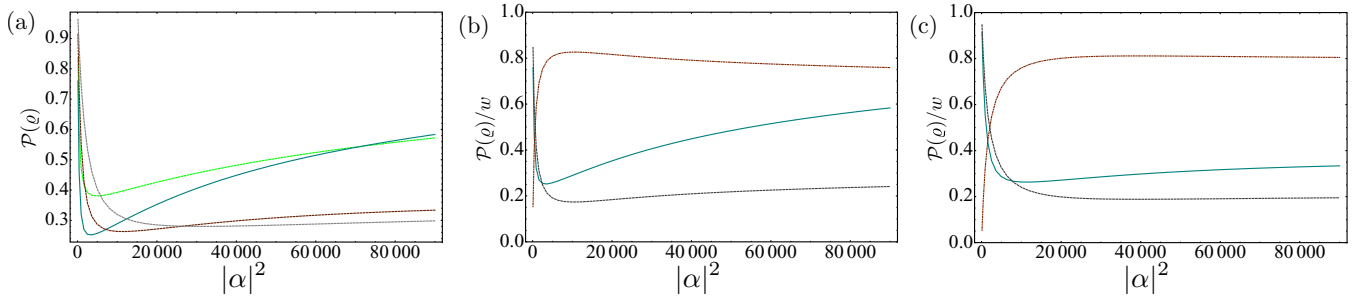

FIG. 8. (Color online) (a) The purity $\mathcal{P}(\varrho) = \mathrm{tr}\{\varrho^2\}$ of the density matrix created by squeezed light [Eq. (50)] with $\omega_1 = 1.47$ eV, $\omega_2 = 1.516$ eV, and $\sigma = 0.014$ eV vs the pump intensity (in units of $\hbar$). The different plots correspond to entanglement times $T_2 - T_1 = 1.452$ $\hbar$/eV (green), 14. 519 $\hbar$/eV (blue), 145.19 $\hbar$/eV (red), and 290.38 $\hbar$/eV (gray). (b) The plot with entanglement time $T_2 - T_1 = 14.519$ $\hbar$/eV of (a) is plotted together with the contribution of the coherent part (dashed), and the incoherent part (dot-dashed) to the entire density matrix. (c) Same as (b) but for $T_2 - T_1 = 290.38$ $\hbar$/eV.

Using Eqs. (19) and (50), we obtain for the coincidence rate

$$S_{ij}(\Gamma) = 1 + \frac{\langle E^\dagger(\omega_{ig})E^\dagger(\omega_{jg})\rangle\langle E(\omega_{ig})E(\omega_{jg})\rangle}{\langle E^\dagger(\omega_{ig})E(\omega_{ig})\rangle\langle E^\dagger(\omega_{jg})E(\omega_{jg})\rangle} + \frac{\langle E^\dagger(\omega_{ig})E(\omega_{jg})\rangle\langle E^\dagger(\omega_{jg})E(\omega_{ig})\rangle}{\langle E^\dagger(\omega_{ig})E(\omega_{ig})\rangle\langle E^\dagger(\omega_{jg})E(\omega_{jg})\rangle}. \quad (52)$$

The first line is again the coherent contribution as discussed in the previous subsection; the second line is analogous to the signal of stochastic light, Eq. (30).

VII. DISCUSSION

We have investigated how properties of light are imprinted in the doubly-excited-state density matrices of multilevel atoms induced by the absorption of classical coherent light, Gaussian stochastic light, two-photon Fock states, and squeezed light. Two-photon states create entangled, pure states, whereas classical coherent light produces product states, and stochastic light yields incoherent mixtures. The differences between the effects of the various fields of the field can be rationalized by the way the interaction with matter affects the quantum fields. After the first interaction with the atoms, the field (31) has evolved into the single-photon state $|\psi'\rangle \propto E|\psi\rangle$. Even for a separable state, this can create a coherent superposition state, $\propto \int d\omega[\Phi_1(\omega) + \Phi_2(\omega)]a^\dagger|0\rangle$. For a classical light, the interaction with matter does not affect the state of light. Tracing out the matter in Eq. (6), we have $\varrho_{\text{field}}(t) = \varrho_{\text{field}}(t_0)$. It will be interesting to test this hypothesis in the future using methods from quantum information theory [52]. Our results suggest that classical light cannot induce nonclassical correlations in the matter system, but this remains to be proved. Most importantly, it will be necessary to identify signatures of classical frequency correlations of light [22] on the created matter density matrices, and whether they can create matrices with nonzero quantum discord. Furthermore, introducing interactions between the atoms opens up the possibility to discuss the entanglement of delocalized quasiparticles, since the excitations can be regarded as interacting bosons [53–55].

We showed that the g_2 function of the incoming light fields can serve as an indicator of the ability of the light to induce correlations between the atoms. Equation (19) reveals that differences between single- and two-photon coincidence measurements result from differences between the two-point and the four-point correlation function of the light. Many photon correlation effects such as the Hong-Ou-Mandel effect may also be traced back to this difference. This suggests an intimate connection between the ability of quantum light to show nonclassical photon correlations, and its ability to excite nonclassical doubly excited states.

ACKNOWLEDGMENTS

We gratefully acknowledge the support of the National Science Foundation through Grant No. CHE-1058791, and the Chemical Sciences, Geosciences and Biosciences Division, Office of Basic Energy Sciences, Office of Science, U.S. Department of Energy.

[1] R. Horodecki, P. Horodecki, M. Horodecki, and K. Horodecki, Rev. Mod. Phys. **81**, 865 (2009).
[2] K. Modi, A. Brodutch, H. Cable, T. Paterek, and V. Vedral, Rev. Mod. Phys. **84**, 1655 (2012).
[3] M. Nielsen and I. Chuang, *Quantum Computation and Quantum Information*, Cambridge Series on Information and the Natural Sciences (Cambridge University Press, Cambridge, UK, 2000).
[4] J. Yuen-Zhou, J. J. Krich, M. Mohseni, and A. Aspuru-Guzik, Proc. Natl. Acad. Sci. (U.S.A.) **108**, 17615 (2011).
[5] O. Roslyak, C. A. Marx, and S. Mukamel, Phys. Rev. A **79**, 033832 (2009).
[6] O. Roslyak and S. Mukamel, Phys. Rev. A **79**, 063409 (2009).
[7] M. Richter and S. Mukamel, Phys. Rev. A **82**, 013820 (2010).
[8] S. Mukamel and M. Richter, Phys. Rev. A **83**, 013815 (2011).
[9] M. Kira, S. W. Koch, R. Smith, A. E. Hunter, and S. Cundiff, Nat. Phys. **7**, 799 (2011).
[10] J. Javanainen and P. L. Gould, Phys. Rev. A **41**, 5088 (1990).
[11] D.-I. Lee and T. Goodson, J. Phys. Chem. B **110**, 25582 (2006).
[12] A. R. Guzman, M. R. Harpham, O. Suzer, M. M. Haley, and T. G. Goodson, J. Am. Chem. Soc. **132**, 7840 (2010).
[13] H.-B. Fei, B. M. Jost, S. Popescu, B. E. A. Saleh, and M. C. Teich, Phys. Rev. Lett. **78**, 1679 (1997).
[14] J. Peřina, Jr., B. E. A. Saleh, and M. C. Teich, Phys. Rev. A **57**, 3972 (1998).
[15] B. E. A. Saleh, B. M. Jost, H.-B. Fei, and M. C. Teich, Phys. Rev. Lett. **80**, 3483 (1998).
[16] L. Upton, M. Harpham, O. Suzer, M. Richter, S. Mukamel, and T. Goodson, J. Phys. Chem. Lett. **4**, 2046 (2013).
[17] F. Schlawin, K. E. Dorfman, B. P. Fingerhut, and S. Mukamel, Phys. Rev. A **86**, 023851 (2012).
[18] H. Oka, J. Chem. Phys. **134**, 124313 (2011).
[19] H. Oka, J. Chem. Phys. **135**, 164304 (2011).
[20] M. G. Raymer, A. H. Marcus, J. R. Widom, and D. L. P. Vitullo, J. Phys. Chem. B **117**, 15559 (2013).
[21] F. Schlawin, K. E. Dorfman, B. P. Fingerhut, and S. Mukamel, Nat. Commun. **4**, 1782 (2013).
[22] R. Kaltenbaek, J. Lavoie, D. N. Biggerstaff, and K. J. Resch, Nat. Phys. **4**, 864 (2008).
[23] K. J. Resch, R. Kaltenbaek, J. Lavoie, and D. N. Biggerstaff, Proc. SPIE **7465**, 74650N (2009).
[24] R. de J León-Montiel, J. Svozilík, L. J. Salazar-Serrano, and J. P. Torres, New J. Phys. **15**, 053023 (2013).
[25] A. Ishizaki and G. R. Fleming, Annu. Rev. Condens. Matter **3**, 333 (2012).
[26] T. Mančal, N. Christensson, V. Lukeš, F. Milota, O. Bixner, H. F. Kauffmann, and J. Hauer, J. Phys. Chem. Lett. **3**, 1497 (2012).

[27] P. Brumer and M. Shapiro, Proc. Natl. Acad. Sci. (U.S.A.) **109**, 19575 (2012).
[28] S. Mukamel, *Principles of Nonlinear Optical Spectroscopy*, Oxford Series on Optical Sciences (Oxford University Press, Oxford, UK, 1999).
[29] N. Morita and T. Yajima, Phys. Rev. A **30**, 2525 (1984).
[30] R. Beach and S. R. Hartmann, Phys. Rev. Lett. **53**, 663 (1984).
[31] U. Harbola and S. Mukamel, Phys. Rep. **465**, 191 (2008).
[32] A. Muthukrishnan, G. S. Agarwal, and M. O. Scully, Phys. Rev. Lett. **93**, 093002 (2004).
[33] Z. Zheng, P. L. Saldanha, J. R. Rios Leite, and C. Fabre, arXiv:1303.5043.
[34] M. Richter and S. Mukamel, Phys. Rev. A **83**, 063805 (2011).
[35] M. Scully and M. Zubairy, *Quantum Optics* (Cambridge University Press, Cambridge, UK, 1997).
[36] R. Glauber, *Quantum Theory of Optical Coherence* (Wiley, New York, 2007).
[37] L. Mandel and E. Wolf, *Optical Coherence and Quantum Optics* (Cambridge University Press, Cambridge, UK, 1995).
[38] C. K. Law, I. A. Walmsley, and J. H. Eberly, Phys. Rev. Lett. **84**, 5304 (2000).
[39] D. Branning, W. P. Grice, R. Erdmann, and I. A. Walmsley, Phys. Rev. Lett. **83**, 955 (1999).
[40] B. Dayan, A. Pe'er, A. A. Friesem, and Y. Silberberg, Phys. Rev. Lett. **94**, 043602 (2005).
[41] B. Dayan, A. Pe'er, A. A. Friesem, and Y. Silberberg, Phys. Rev. Lett. **93**, 023005 (2004).
[42] Y. Shih, IEEE J. Sel. Top. Quantum Electron. **9**, 1455 (2003).
[43] O. Aytür and P. Kumar, Phys. Rev. Lett. **65**, 1551 (1990).
[44] A. Fraine, O. Minaeva, D. S. Simon, R. Egorov, and A. V. Sergienko, Opt. Lett. **37**, 1910 (2012).
[45] N. Uribe-Patarroyo, A. Fraine, D. S. Simon, O. Minaeva, and A. V. Sergienko, Phys. Rev. Lett. **110**, 043601 (2013).
[46] H. Breuer and F. Petruccione, *The Theory of Open Quantum Systems* (Oxford University Press, Oxford, UK, 2002).
[47] D. T. Smithey, M. Beck, M. Belsley, and M. G. Raymer, Phys. Rev. Lett. **69**, 2650 (1992).
[48] A. I. Lvovsky and M. G. Raymer, Rev. Mod. Phys. **81**, 299 (2009).
[49] A. Christ, K. Laiho, A. Eckstein, K. N. Cassemiro, and C. Silberhorn, New J. Phys. **13**, 033027 (2011).
[50] A. Christ, B. Brecht, W. Mauerer, and C. Silberhorn, New J. Phys. **15**, 053038 (2013).
[51] F. Schlawin and S. Mukamel, J. Phys. B **46**, 175502 (2013).
[52] F. Mintert, A. R. Carvalho, M. Kuś, and A. Buchleitner, Phys. Rep. **415**, 207 (2005).
[53] M. C. Tichy, F. Mintert, and A. Buchleitner, J. Phys. B **44**, 192001 (2011).
[54] M. C. Tichy, P. A. Bouvrie, and K. Mølmer, Phys. Rev. Lett. **109**, 260403 (2012).
[55] S. Mukamel, J. Chem. Phys. **132**, 241105 (2010).